

ALIGNED VECTOR QUANTIZATION FOR EDGE-CLOUD COLLABORATIVE VISION-LANGUAGE MODELS

Xiao Liu¹ Lijun Zhang¹ Deepak Ganesan¹ Hui Guan¹

ABSTRACT

Vision Language Models (VLMs) are central to Visual Question Answering (VQA) systems and are typically deployed in the cloud due to their high computational demands. However, this cloud-only approach under-utilizes edge computational resources and requires significant bandwidth for transmitting raw images. In this paper, we introduce an edge-cloud collaborative VQA system, called LLaVA-AlignedVQ, which features a novel Aligned Vector Quantization algorithm (AlignedVQ) that efficiently compress intermediate features without compromising accuracy to support partitioned execution. Our experiments demonstrate that LLaVA-AlignedVQ achieves approximately $1365\times$ compression rate of intermediate features, reducing data transmission overhead by 96.8% compared to transmitting JPEG90-compressed images to the cloud. LLaVA-AlignedVQ achieves an inference speedup of $2\text{-}15\times$ while maintaining high accuracy, remaining within -2.23% to $+1.6\%$ of the original model’s accuracy performance across eight VQA datasets, compared to the cloud-only solution.

1 INTRODUCTION

Visual Question Answering (VQA) systems allow machines to respond to natural language questions based on visual inputs. They have numerous practical applications, including assistive technologies for visually impaired individuals, real-time video analytics, and human-computer interaction (Singh et al., 2023). Recent advancements in Vision Language Models (VLMs) (Alayrac et al., 2022; Li et al., 2023a; Liu et al., 2023) have greatly enhanced VQA capabilities, making VLMs the core component of these systems. A typical VLM architecture includes a transformer-based vision encoder for processing visual inputs, a visual-text alignment adaptor that maps visual features to the textual domain for improved joint understanding, and a Large Language Model (LLM) that generates the answer.

VLMs are typically deployed in the cloud due to their substantial computational requirements. For instance, LLaVA, a leading VLM, uses CLIPViT-large-336 as visual encoder, which demands approximately 167.45 GMACs per forward pass, making it challenging to run efficiently on resource-constrained edge devices. While using a smaller vision encoder could reduce computational needs, this often results in significant performance degradation, especially for tasks requiring precise visual-text alignment (Lin et al., 2024; Liu et al., 2024b). This problem is compounded by the

much more intensive resource requirements of LLaVA’s LLM component.

This cloud-only approach, however, has two main limitations. First, it under-utilizes the computing power of edge devices, especially those already equipped with AI capabilities. Second, it requires transmitting raw images to the cloud, assuming high bandwidth availability to achieve low inference latency. Compression methods like JPEG can alleviate this issue by reducing transmission overhead but compromise task accuracy in the process. As compression rates increase to fit lower transmission bandwidths, accuracy declines significantly. Figure 1 illustrates this trade-off, where the blue curve (LLaVA-JPEG) showing the accuracy of the LLaVA model with the Vicuna-7B backbone (Chiang et al., 2023) on the VQA-v2 dataset (Goyal et al., 2017) when input images undergo JPEG compression at various compression rates. Higher compression rates reduce the data size for transmission, lowering the inference latency, but incur a notable 6.54% accuracy drop comparing to the original LLaVA model (LLaVA-Ori).

In this paper, we address these limitations with a partitioned execution approach, where the initial layers of the VLM’s visual encoder run locally when edge resources permit, while the remaining layers of the visual encoder and the other VLM components execute in the cloud. This partitioned execution allows the VQA system to shift some processing from the cloud to edge devices, reducing strain on cloud infrastructure and associated costs. It can also benefit from task-aware compression on intermediate features from the visual encoder, minimizing transmission overhead and po-

¹Manning College of Information and Computer Sciences, University of Massachusetts, Amherst, Massachusetts, USA. Correspondence to: Xiao Liu <xiaoliu1990@cs.umass.edu>.

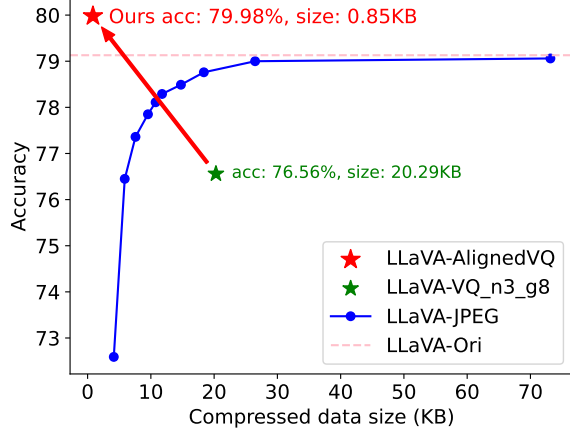


Figure 1: Accuracy with compressed data size for different variants of LLaVA on the VQA-v2 dataset. Our approach, LLaVA-AlignedVQ (marked by the red star), achieves a high accuracy of 79.98% with a minimal transmission size of 0.85KB, balancing accuracy and compression efficiency.

tentially outperforming generic methods like JPEG on raw images. Task-aware compression customizes the compression of intermediate features specifically for the VQA task. Unlike JPEG-like generic compression algorithms, which aim to retain as much of the raw image as possible without considering downstream tasks, task-aware compression are specifically optimized on the question answering task, offering opportunities for efficient compression without sacrificing task accuracy.

The basic idea poses a critical research challenge: designing a task-aware compression algorithm that achieves high compression rates while preserving VQA accuracy. This compression algorithm must satisfy three essential criteria: (1) it should provide a high compression rate to reduce transmission overhead, (2) it must execute quickly to avoid adding runtime overhead during VLM inference, and (3) it should be easily adaptable to the VQA task using a VQA training dataset to maintain task accuracy.

While Vector Quantization (VQ) is a promising candidate thanks to its high compression rates and efficient computation, applying it to compress intermediate features from the VLM’s visual encoder results in substantial accuracy loss. The green star in Figure 1 shows the best VQA accuracy on the VQA-v2 dataset achieved by an advanced VQ variant that combines Residual VQ (Zeghidour et al., 2021) and Grouped VQ (Yang et al., 2023) with 3 codebooks and 8 groups. Despite this, the method still underperforms compared to transmitting JPEG-compressed raw images in a cloud-only setup, highlighting the need for a more advanced compression approach that can reduce transmission overhead without sacrificing accuracy.

To address the challenge, we propose AlignedVQ (Aligned Vector Quantization), a task-aware compression algorithm that is lightweight, achieves high compression rates, and preserves task accuracy. AlignedVQ injects a VQ module after normalization layers to mitigate the accuracy drops caused by quantization error, since the intermediate features generated by these layers exhibit a lower coefficient of variation, which is more suitable for quantization. It also introduces a lightweight adaptor, *Dual Linear Projection (DLP)*, within the VQ module to align the features before and after quantization. To further enhance task accuracy, AlignedVQ finetunes the VQ codebook, the DLP adaptor, and the LoRA adaptor in the LLM part of the VLM together. AlignedVQ allows the visual encoder to be partitioned at any transformer blocks, enabling flexibly shifting variable amount of VQA processing on edge devices.

We implement AlignedVQ on top of LLaVA-1.5 (Liu et al., 2024a), a state-of-the-art VLM, resulting in LLaVA-AlignedVQ, and evaluate its performance across eight datasets. LLaVA-AlignedVQ reduces data transmission size by up to $1365\times$, a 96.8% reduction in transmission size compared to sending JPEG90-compressed images, while maintaining task accuracy within -2.23% to $+1.6\%$ of the original model performance. The red star in Figure 1 highlights that LLaVA-AlignedVQ can achieve extreme compression rates with even higher task accuracy compared to the original LLaVA model (LLaVA-Ori) on the VQA-v2 dataset.

We further build an edge-cloud collaborative VQA system that executes the first block of the visual encoder and the quantization module of LLaVA-AlignedVQ on NVIDIA Jetson AGX Xavier and the rest of LLaVA-AlignedVQ on a workstation with an A100 GPU. Evaluation demonstrates that LLaVA-AlignedVQ achieves $2 - 15\times$ speedups in executing the visual encoder under different transmission bandwidth compared to the cloud-only solution using JPEG90-compressed images. The execution overhead of the compression takes 4.91ms per sample, accounting for 25% of the local execution time.

We summarize our contributions as follows:

- We propose AlignedVQ, a task-aware compression algorithm that incorporates post-normalization vector quantization, Dual Linear Projection, and LoRA fine-tuning to achieve high compression rates, minimal computational overhead, and high task accuracy.
- We implement AlignedVQ on top of LLaVA-1.5 and evaluate its superior performance across various VQA datasets.
- We develop an edge-cloud collaborative VQA system that leverages partitioned execution to address the limitations of cloud-only solutions and demonstrate the benefits of partitioned execution in reducing execution

latency.

2 BACKGROUND AND MOTIVATIONS

In this section, we provide the necessary background on Vector Quantization (VQ), which AlignedVQ builds on, and motivate our approach.

2.1 Vector Quantization (VQ)

VQ compresses high-dimensional data by mapping continuous feature vectors to a discrete set of values (Gersho & Gray, 2012). We first introduce Vanilla VQ and then its variants Residual VQ and Grouped VQ.

Vanilla VQ partitions the feature space into clusters, where each data point is assigned to its nearest cluster centroid. Let the codebook $\mathbf{e} \in \mathbb{R}^{K \times D}$ represents the set of centroids, where K is the number of centroids and D is the feature dimension. We define VQ with the codebook \mathbf{e} as $\mathcal{Q}_{\mathbf{e}}$. For an input vector $\mathbf{z} \in \mathbb{R}^D$, VQ maps \mathbf{z} to a discrete index i by selecting the nearest centroid in the codebook,

$$i = \arg \min_i \|\mathbf{e}_i - \mathbf{z}\|_2^2. \quad (1)$$

Thus, the quantization operation is represented as $\mathcal{Q}_{\mathbf{e}}(\mathbf{z}) = \mathbf{e}_i$, where \mathbf{e}_i is the nearest centroid. This process reduces data size by transmitting only the index i rather than the full feature vector \mathbf{z} . To obtain the trained codebook \mathbf{e} in VQ, we can perform K -means clustering on a set of embeddings $\mathbf{Z} \in \mathbb{R}^{N \times D}$ in the feature space, using the centroids of these clusters as the codebook entries. These centroids can also be updated online with an exponential moving average strategy (Van Den Oord et al., 2017).

Residual VQ (Zeghidour et al., 2021) improves Vanilla VQ by applying multiple stages of quantization. At each stage, the residuals, which are the differences between the original feature vectors and the quantized vectors, are further quantized with a new codebook. By progressively refining the residuals, Residual VQ can reduce the quantization error compared to the vanilla one. **Grouped VQ** (Yang et al., 2023) splits feature vectors into smaller groups and applies VQ independently within each group. By quantizing smaller feature subsets, it reduces the computation complexity and quantization errors.

2.2 Motivations and Challenges

In this work, we explore the application of VQ in compressing intermediate features of the vision encoder in pretrained Vision-Language Models (VLMs). It is motivated by the observation that VQ can dramatically lower the data size to transmit with a low computation overhead.

Assume that the vision encoder uses a transformer architecture, the size of the intermediate feature from a transformer block is $[B, N, C]$, where B is the batch size, N is the num-

ber of visual tokens, and C is the channel size. The total number of bits required for these features is $B \times N \times C \times K$ with K -bit representation for each value. By applying VQ, we compress the feature by transmitting only the indices of the corresponding codebook entries. Assuming the codebook has 2^m rows, each of dimension C , the index for each token can be represented by a m -bit integer. The total number of bits required to represent the features is $B \times N \times m$, which has a compression rate of $\frac{C \times K}{m}$. To make it concrete, in the ViT-large-336 model, where C is typically 1024, this results in an extremely high compression rate of nearly $1365\times$ with $K = 16$ and $m = 12$. The compression process is also very lightweight as the quantization computation is essentially one dense matrix-matrix multiplication.

While VQ effectively reduces transmission overhead, it introduces a new challenge: *mitigating the significant accuracy loss that can occur when applying VQ within the visual encoder of VLMs*.

Vanilla VQ causes significant accuracy drops. A straightforward approach of using VQ for feature compression is to compress the intermediate features between adjacent transformer blocks. However, this naive approach results in a severe drop in accuracy. In Figure 2c, we present the accuracy results on the VQA-v2 dataset (Goyal et al., 2017) using LLaVA with Vanilla VQ applied after different transformer blocks. Compared to the accuracy 79.13% of the original LLaVA model (i.e., the pink dashed line), applying VQ results in an accuracy drop of 10.51% to 37.94% across different blocks (i.e., the blue line). What’s worse, the earlier the partitioning point in the model, the greater the accuracy drop.

VQ variants with less quantization errors cannot mitigate the accuracy gaps. We also explored other VQ variants, such as Residual VQ and Grouped VQ introduced in Section 2.1, to mitigate this accuracy loss as they reduce quantization errors. As shown in Figures 2a and 2b, we experimented with different numbers of codebooks for Residual VQ and various number of groups for Grouped VQ. While these variants improved accuracy from the range of 41.19% – 68.62% to 72.65% – 73.75% with more codebooks, and to 71.15% – 73.34% with more groups, a significant gap of 5.38% – 7.98% still remains between the VQ-applied models and the original model. Moreover, these VQ variants come at the cost of increased compressed feature size, thereby more transmission overhead. Specifically, with n codebooks and g group, the compressed feature size is enlarged by $n \times g$.

We further experimented with a combination of Residual VQ and Grouped VQ, shown as the green line in Figure 2c. When using 3 codebooks and 8 groups, accuracy was consistently improved across blocks, resulting in an accuracy drop of 2.57% – 5.68% compared to the original model.

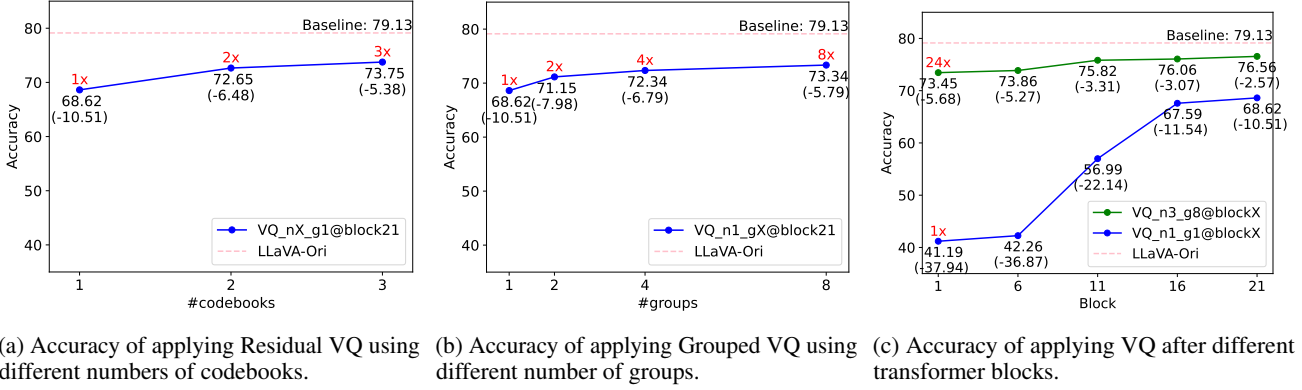


Figure 2: Accuracy performance of LLaVA on VQA-v2 datasets with different VQ variants. (a) Residual VQ with different codebooks (b) Grouped VQ with different number of groups, and (c) Vanilla VQ (blue) and the combined VQ with 3 codebooks and 8 groups (green). *LLaVA-Ori*: the baseline, i.e., the original LLaVA accuracy. *VQ_{np-gq@blockX}*: the accuracy when using VQ with p codebook and q group after the X th transformer block. $n\times$ in red: the multiple by which the compressed data size increases as the number of codebook and groups grows.

This combined VQ variant still cannot fully bridge the gap. Besides, it comes with the additional cost of a $24\times$ larger compressed feature size than the Vanilla VQ with only 1 codebook and 1 group.

3 DESIGN OF ALIGNEDVQ

We propose AlignedVQ, a lightweight and effective compression algorithm designed to mitigate accuracy loss while retaining the compression benefits of Vanilla VQ. By applying AlignedVQ to compress intermediate features from the vision encoder in the pretrained VLM, the partitioned model achieves lower inference latency thanks to reduced data transmission overhead, while preserving high accuracy compared with cloud-only solutions.

3.1 Overview

Figure 3 illustrates the architecture and workflow of an VLM with the proposed AlignedVQ for efficient edge-cloud collaborative execution. The VLM consists of a vision encoder equipped with an AlignedVQ module, a projector for modality alignment, and a language model that interprets question embeddings and generates language responses. AlignedVQ allows the visual encoder to be partitioned at any transformer blocks, enabling flexibly shifting variable amount of VQA processing on edge devices. The overall workflow is divided into two main stages, training and deployment. The key design features of AlignedVQ are detailed in Section 3.2.

Training Stage. The offline training stage prepares the VLM model for partitioned execution by fine-tuning the AlignedVQ module to adapt to the specific VQA dataset. AlignedVQ employs a codebook that maps continuous fea-

ture vectors to discrete indices, with the codebook being iteratively updated using moving average as described in Section 2.1. After quantization, the indices are immediately converted back into their corresponding features from the codebook, and the gradients from the pre-quantization features are propagated to the quantized features to maintain the gradient chain. In addition to the codebook, AlignedVQ also fine-tunes a Dual Linear Projection (DLP) module that places gated linear projections before and after quantization, along with the LoRA parameters in the LLM to improve task accuracy.

Deployment Stage. In the deployment stage, the VLM is partitioned between the edge and the cloud. The edge device processes the initial layers of the visual encoder up to the AlignedVQ module to generate intermediate features. These features are then quantized by the AlignedVQ module executed locally, transmitting only the codebook indices to the cloud. On the cloud, the transmitted indices are decoded back into intermediate features using the same codebook, after which they proceed through the remaining components of the VLM.

3.2 The AlignedVQ Algorithm

We now detail the three key design features of AlignedVQ that enable it to achieve a high compression rate while preserving task accuracy.

3.2.1 Normalized Feature Compression

AlignedVQ partitions the visual encoder of a VLM by inserting Vector Quantization (VQ) immediately after the normalization layers within a transformer block. This design choice is motivated by a fundamental connection between

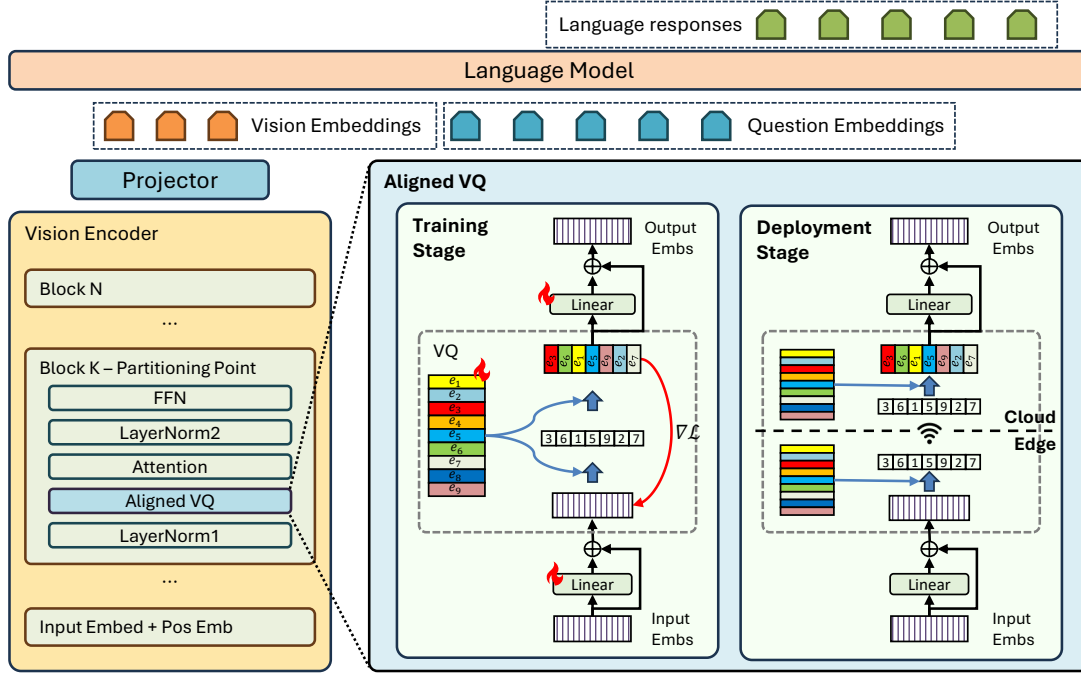


Figure 3: Overview of the Vision Language Model (VLM) with the proposed AlignedVQ. The model consists of a Vision Encoder, a proposed AlignedVQ module, a Projector, and a Language Model. During training, continuous features from the Vision Encoder are quantized with AlignedVQ and iteratively updated with back-propagation. When deployment, only quantized indices are transmitted from edge to cloud, minimizing data transfer while preserving high accuracy.

layer normalization and vector quantization: VQ’s effectiveness depends on its ability to approximate a continuous feature space with a discrete set of codebook vectors, and layer normalization creates precisely the kind of structured feature space that VQ can represent efficiently.

As illustrated in Figure 3, a typical transformer block consists of four main components: the first layer normalization (LN1), the attention module (ATTN), the second layer normalization (LN2), and the feed-forward network (FFN). While VQ could theoretically be inserted after any of these layers, the features after normalization layers have a crucial property - they are standardized to lie approximately on a hypersphere with controlled statistical properties. In contrast, the outputs of ATTN and FFN can occupy a much less constrained space with highly variable magnitudes. Figure 4 visualizes the histogram of the magnitudes of the feature vectors from LN1, ATTN, LN2, and FFN, reflecting the magnitude distribution difference of these layers.

This difference proves critical for VQ’s performance. When quantizing normalized features, the codebook only needs to capture variations in direction on the hypersphere, rather than variations in both direction and magnitude. Table 1 demonstrates this effect empirically: applying VQ after LN1 and LN2 results in minimal accuracy drops of 0.11% and 0.4%, while applying it after ATTN and FFN leads to

Table 1: Accuracy for different VQ insertion locations. LLaVA-Ori represents the original model without VQ.

Location	LN1	ATTN	LN2	FFN	LLaVA-Ori
Accuracy	79.02	66.17	78.73	68.62	79.13

much larger drops of 12.96% and 10.51% respectively (see Section 4.5 for more comparison).

We can quantify this structural difference in the feature spaces using the coefficient of variation (CV) (Abdi, 2010), which is defined as the ratio of the standard deviation to the mean. Figure 4 presents the CV of different layers to measure the relative dispersion of feature magnitudes. It is shown that features after normalization layers have significantly lower CVs, indicating they lie more consistently near the surface of a hypersphere. This well-structured geometry makes them inherently more amenable to efficient quantization, explaining the significant performance difference in accuracy when VQ is applied on the normalized features and the unnormalized ones in the transformer block.

3.2.2 Dual Linear Projection

AlignedVQ includes Dual Linear Projection (DLP) to ad-

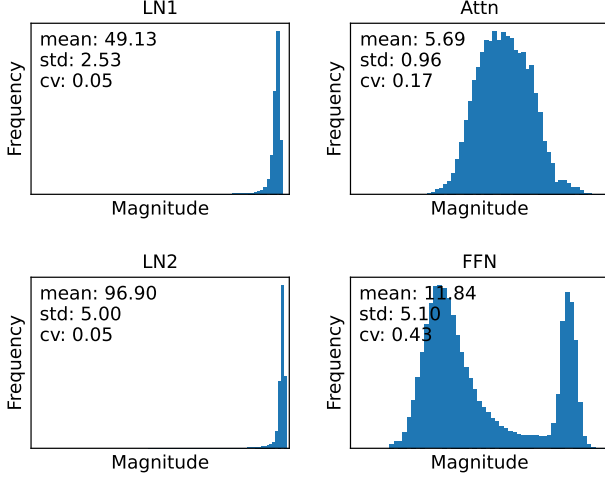


Figure 4: Histograms of feature magnitudes for different locations within a transformer block. The normalized layers (LN1 and LN2) have lower coefficient of variation (CV) values, indicating tighter distributions around the mean, making quantization more effective. In contrast, intermediate features from ATTN and FFN layers show higher variability.

dress a fundamental challenge in applying VQ to pretrained networks: feature distribution shift. In a pretrained model, each layer is optimized to process features with specific statistical properties. When we insert VQ between layers, even small changes in these properties can cascade into significant accuracy drops, as the subsequent layers receive inputs that deviate from their training distribution.

DLP addresses this challenge through a pair of learned transformations that act as “adapters” before and after quantization. The input projection helps shape features into a more quantization-friendly form while preserving their semantic content. The output projection then helps restore the statistical properties that downstream layers expect. Formally, VQ with DLP is defined as,

$$\begin{aligned} \mathbf{Z}_q &= VQ(\mathbf{Z}_{in} + \tanh(\gamma_{in}) \cdot \text{Linear}(\mathbf{Z}_{in})) \\ \mathbf{Z}_{out} &= \mathbf{Z}_q + \tanh(\gamma_{out}) \cdot \text{Linear}(\mathbf{Z}_q), \end{aligned} \quad (2)$$

where \mathbf{Z}_{in} is the intermediate features from the last layer, \mathbf{Z}_q is the quantized features, and \mathbf{Z}_{out} is the recovered features as the inputs for the next layer. γ_{in} and γ_{out} are learnable parameters initialized to zero, which are controlling factors for rescaling the outputs of the linear projections.

This approach is particularly effective because it separates two concerns: the VQ module can focus on achieving high compression ratios, while the DLP layers handle the subtle adjustments needed to keep the quantized features compatible with the pretrained model. In Section 4.5, we show that

this division of labor consistently improves task accuracy across all partitioning points, with particularly strong gains in early layers where feature alignment is most critical.

3.2.3 Training Strategy

To further enhance task accuracy, AlignedVQ fine-tunes the LoRA parameters in the LLM of a VLM alongside the VQ codebook and the DLP layers. Mathematically, in a neural network represented by a mapping function $F(x)$ where VQ is applied to quantize the intermediate features \mathbf{Z} , a commitment loss (Van Den Oord et al., 2017) is introduced to encourage \mathbf{Z} to move closer to its corresponding centroid. The overall loss function for finetuning the trainable parameters is:

$$\mathcal{L} = \hat{\mathcal{L}}(F(x)) + \beta \|\mathbf{Z} - \text{sg}(\mathcal{Q}_e(\mathbf{Z}))\|_2^2, \quad (3)$$

where $\hat{\mathcal{L}}$ is the task loss, sg represents the stop gradient operation, and β is a scaling factor for the commitment loss. In Section 4.5, we demonstrate that fine-tuning the LoRA parameters further enhances model’s performance, with a notable accuracy boost of 0.50–0.61%.

3.3 The LLaVA-AlignedVQ Implementation

We implement AlignedVQ on top of the LLaVA-1.5 model (Liu et al., 2024a), a state-of-the-art VLM designed for VQA tasks with outstanding performance. It employs a pretrained CLIPViT (Radford et al., 2021) as the vision encoder, an MLP projection for aligning visual and textual information, and a well-trained Vicuna-7B (Chiang et al., 2023) with a LoRA adaptor for generating answers.

By default, LLaVA-AlignedVQ utilizes a single codebook with 4096 entries of 1024-dimensional features as CLIPViT’s intermediate features has 1024 channels. We evaluate the impacts of different number of codebooks and groups on the performance of LLaVA-AlignedVQ in Section 4.5. LLaVA-AlignedVQ is fine-tuned for one epoch with the Adam optimizer (Kingma, 2014). The training dataset used for training LLaVA-1.5, which is a mixture of multiple datasets, is used to update the codebook and trainable parameters, including Dual Linear Projection and LoRA. The 1-epoch finetuning takes 20h on 4 A100 machine.

AlignedVQ can be applied to any block within the visual encoder of LLaVA, with optimal partitioning points depending on the specific optimization objectives. Here, we focus on optimizing inference latency. For this purpose, LLaVA-AlignedVQ applies VQ immediately after the first normalization layer of the first block of the visual encoder. We evaluate the impacts of different partition points on the performance of LLaVA-AlignedVQ at Section 4.5. In CNNs, it is often possible to find a partitioning point with relatively small intermediate feature sizes. However, transformer models generally have consistent computational cost

and intermediate feature sizes across blocks, meaning that edge computation time increases linearly as the partitioning point moves deeper into the model, while transmission time remains constant. Therefore, from a latency-optimization perspective, the best strategy for applying VQ to compress intermediate features in transformer models is to partition as early as possible.

4 EXPERIMENTS

Our experiments aim to answer the following questions: **Q1:** How is the task accuracy of LLaVA-AlignedVQ compared to the original LLaVA model and alternative approaches? (§ 4.2) **Q2:** How is the data compression rates of LLaVA-AlignedVQ compared to alternative approaches? (§ 4.3) **Q3:** How is the execution latency of LLaVA-AlignedVQ compared to the cloud-only alternative at various network bandwidth settings? (§ 4.4) **Q4:** How does model partitioning points, each design features of AlignedVQ, and quantization hyperparameters affect the performance of LLaVA-AlignedVQ? (§ 4.5)

4.1 Experimental Settings

Benchmarks. We evaluate LLaVA-AlignedVQ on eight diverse Vision Question Answering (VQA) benchmarks: **VQA-v2** (Goyal et al., 2017) and **GQA** (Hudson & Manning, 2019) for open-ended questions, **VizWiz** (Gurari et al., 2018) for questions from visually impaired users, **TextVQA** (Singh et al., 2019) for text-rich queries, **POPE** (Li et al., 2023b) for model’s degree of hallucination on three sampled subsets of COCO (Lin et al., 2014), random, common, and adversarial, **MMBench** (Liu et al., 2025) for all-round shuffling on multiple choice answers, **LLaVA-Wild** (Liu et al., 2023) and **MM-Vet** (Yu et al., 2023) for visual conversations on a diverse range of tasks. POPE reports F1 Score, LLaVA-Wild and MM-Vet utilize the answer score evaluated by GPT-4o (Achiam et al., 2023), and all the other datasets use accuracy. LLaVA-AlignedVQ uses the same codebook to compress intermediate feature for all these benchmarks.

Alternatives for Comparison. We compare the accuracy and latency of **LLaVA-AlignedVQ** against the following alternative approaches:

- **LLaVA-Ori:** Transmits raw images directly to the cloud for processing, with all computations handled on the cloud side.
- **LLaVA₁₊:** An advanced version of LLaVA, in which the LoRA parameters of the pretrained model are further fine-tuned on clean images for an additional epoch, matching the training duration of LLaVA-AlignedVQ.
- **LLaVA-JPEG:** Reduces transmission overhead by sending JPEG-compressed images to the cloud at vary-

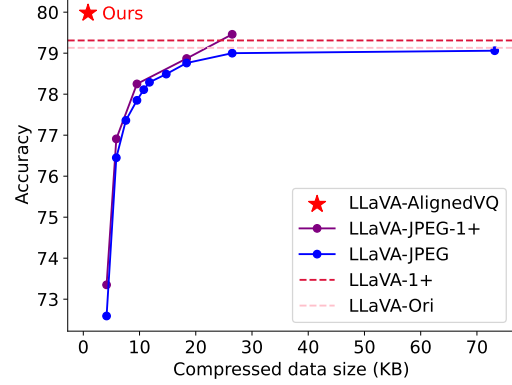


Figure 5: The trade-off between VQA task accuracy and compressed data size on the VQA-v2 dataset.

ing quality levels.

- **LLaVA-JPEG₁₊:** An advanced version of LLaVA-JPEG, where the LoRA parameters are fine-tuned on JPEG-compressed images for an additional epoch, matching the training duration of LLaVA-AlignedVQ.

4.2 Performance on VQA task Accuracy

Figure 5 illustrates the trade-off between VQA task accuracy and compressed data size on the VQA-v2 dataset, presenting an expanded set of baselines compared to Figure 1. Overall, LLaVA-AlignedVQ achieves the lowest transmission overhead while effectively preserving accuracy performance.

Table 2 presents accuracy comparisons across eight VQA datasets. Since the task accuracy of LLaVA-JPEG and LLaVA-JPEG₁₊ are affected by the quality level settings of JPEG algorithms, we present LLaVA-JPEG-10 and LLaVA-JPEG-90, who use the JPEG compression at quality level 10 and 90 respectively, in the table. Same applies to LLaVA-JPEG-10₁₊ and LLaVA-JPEG-90₁₊.

We make two main observations. *First, LLaVA-AlignedVQ consistently demonstrates high accuracy, staying within -2.23% to $+1.6\%$ of the original LLaVA model and -0.86% to $+1.82\%$ of LLaVA₁₊, achieving seven top two accuracy among the eleven results* Although the variants LLaVA-JPEG-90 and LLaVA-JPEG-90₁₊ achieve competitive high accuracy, lower than LLaVA-AlignedVQ by approximately -0.16% and -0.66% on average, they incur a larger transmission overhead as indicated in Table 3, leading to longer inference latency as shown in Section 4.4. Although using JPEG-10 greatly reduces the transmission overhead compared to JPEG-90, from 26.47KB to 4.14KB per sample as reported in Table 3, it suffers from a significant accuracy drop of 5.09% on average.

Second, models fine-tuned with compressed images or compressed intermediate features, such as LLaVA-AlignedVQ and LLaVA-JPEG-90₁₊, achieve even higher accuracy than

Table 2: Accuracy comparison across eight VQA benchmarks. We compare the performance of LLaVA-Ori (original), LLaVA-Ori₁₊ (fine-tuned for one additional epoch), LLaVA-JPEG (evaluate directly on JPEG-compressed images) and LLaVA-JPEG₁₊ (fine-tuned for one additional epoch on JPEG-compressed images) at compression levels of 10 and 90, and the proposed LLaVA-AlignedVQ. The Δ rows indicate the accuracy difference between LLaVA-AlignedVQ and LLaVA-Ori/LLaVA-Ori₁₊. The best two results are bolded and underlined.

Method	VQAv2	GQA	VisWiz	TextVQA	POPE			MMBench		LLaVA-Wild	MM-Vet
					rand	pop	adv	en	cn		
LLaVA-Ori	79.13	62.98	47.78	58.21	87.71	86.72	84.72	66.67	58.93	61.1	30.9
LLaVA ₁₊	79.31	<u>63.53</u>	47.38	56.24	<u>87.84</u>	86.39	84.65	65.64	57.56	<u>61.6</u>	31.9
LLaVA-JPEG-10	72.59	59.54	47.75	50.58	81.02	79.78	77.71	64.17	54.46	54.3	26.9
LLaVA-JPEG-10 ₁₊	73.35	59.99	43.29	49.94	85.11	83.14	80.23	63.05	54.20	51.5	28.5
LLaVA-JPEG-90	79.00	62.44	48.37	57.89	87.53	86.42	84.57	66.32	<u>58.59</u>	60.9	<u>31.1</u>
LLaVA-JPEG-90 ₁₊	<u>79.46</u>	63.06	43.61	56.56	87.81	86.54	84.50	67.09	<u>57.30</u>	61.0	30.7
LLaVA-AlignedVQ	79.98	63.70	47.25	<u>58.06</u>	88.49	86.79	85.16	65.37	56.70	62.7	30.7
Δ LLaVA-Ori	+0.85	+0.72	-0.53	-0.15	+0.78	+0.07	+0.44	-1.30	-2.23	+1.6	-0.2
Δ LLaVA ₁₊	+0.67	+0.17	-0.13	+1.82	+0.65	+0.40	+0.51	-0.27	-0.86	+1.1	-1.2

models fine-tuned on raw images, such as LLaVA₁₊. Specifically, fine-tuning with the raw images for one additional epoch, i.e., LLaVA₁₊, leads to an accuracy drop of 1.2% on average. While LLaVA-AlignedVQ shows accuracy improvements of 0.85% on VQA-v2, 0.72% on GQA, and 0.78%, 0.07%, 0.44% on POPE-rand, POPE-pop, POPE-adv respectively, while LLaVA-JPEG-90₁₊ achieves gains of 0.33% on VQA-v2 and 0.08% on GQA. We hypothesize that this improvement comes from the augmentation effects of compressed data during fine-tuning. When fine-tuning the LoRA parameters in the original LLaVA model for an additional epoch, the model revisits the same data without acquiring new information, may cause overfitting on the train data. In contrast, fine-tuning with compressed data, either images or features, exposes the model to more diverse input space, thereby enhancing accuracy.

4.3 Performance on Data Compression Rates

Table 3 summarizes compressed data size and the compression rates of AlignedVQ and alternative approaches. The raw image resolution is 336×336 , which is the required dimension for the visual encoder CLIPViT-large-336 in LLaVA. For intermediate features, CLIPViT-large-336 produces 577 visual tokens with a dimension of 1024, stored in 16-bit floating point format. For JPEG compression, we evaluated both a commonly-used quality level of 90 and a more aggressive level of 10, offering higher compression with greater quality loss (JPEG-10 and JPEG-90 in Table 3). For compressing intermediate features, we compared AlignedVQ with two extreme cases, 1-bit quantization and an autoencoder that reduce the feature dimension to 1 (1-Bit Quantization and 1-Dim Autoencoder in Table 3).

Table 3: Comparison of compression methods for data transmission in edge-cloud collaborative VQA. We show the raw sizes for images and intermediate features, with various compression methods including JPEG-90 and JPEG-10 for images, 1-Bit Quantization, 1-Dimensional Autoencoder, and AlignedVQ for features.

Raw Size (KB)	Image (336×336)		Intermediate Features (1, 577, 1024)		
	330.75		1154		
Compression Method	JPEG-90	JPEG-10	1-Bit Quantization	1-Dim Autoencoder	AlignedVQ
Size (KB)	26.47	4.14	72.125	1.127	0.845
Compression Rate (X)	12.49	79.89	16	1024	1365

Overall, AlignedVQ achieves the lowest transmission overhead of 0.845KB per sample, leading to the highest compression rate of $1365\times$. Compared with JPEG-compressed images, AlignedVQ reduces transmission overhead by 96.8% ($1 - 0.845/26.47$) relative to JPEG-90 and 79.6% ($1 - 0.845/4.14$) relative to JPEG-10. In contrast, bit quantization, which compresses each value independently, cannot match AlignedVQ’s high compression rate. While autoencoders can reduce feature dimensions to the extreme (e.g., to 1), such heavy compression often compromises task performance by discarding crucial feature details (Berahmand et al., 2024). AlignedVQ, however, achieves high compression while maintaining accuracy.

4.4 Performance on Inference Latency

We evaluate LLaVA-AlignedVQ using an NVIDIA Jetson AGX Xavier as the edge device and a workstation equipped with an A100 GPU as the cloud server. To simulate various network conditions, we measure the inference latency of

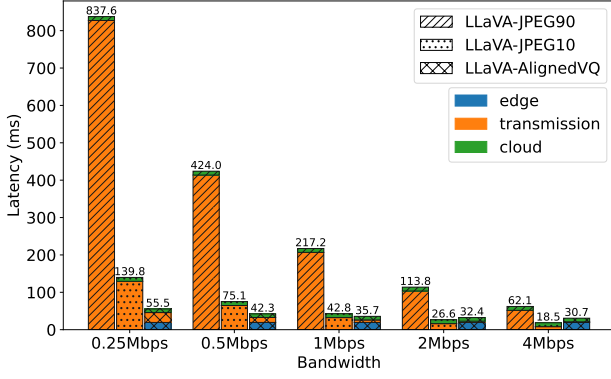


Figure 6: The inference latency of the visual encoder for LLaVA-AlignedVQ, and the two cloud-only solutions, LLaVA-JPEG90 and LLaVA-JPEG10, under different transmission bandwidth.

LLaVA-AlignedVQ’s visual encoder under different transmission bandwidths, ranging from 0.25Mbps to 4Mbps. We compare the inference latency of our edge-cloud collaborative solution, LLaVA-AlignedVQ, with two cloud-only approaches, LLaVA-JPEG-90 and LLaVA-JPEG-10, which transmit JPEG-compressed images.

Figure 6 reports the inference latency, including the edge computation time, the transmission time, and the cloud execution time. For LLaVA-JPEG variants, the edge computation time is ignored as JPEG compression usually takes less than 1ms with proper optimization. Since the large language model is executed on the cloud in all setups, its execution time is excluded from this comparison. Overall, LLaVA-AlignedVQ achieves an inference speedup of 2-15 \times compared to the cloud-only solution using JPEG90-compressed images. Against JPEG10-compressed images, our solution still provides a 1.19-2.52 \times inference speedups at poor bandwidth conditions (0.25-1 Mbps). Although JPEG-10 compression is competitive in latency, it compromises accuracy as highlighted in Section 4.2.

Overhead of Local Compression. LLaVA-AlignedVQ introduces a quantization operation for data compression, which introduces compression overhead during VQA processing. Specifically, LLaVA-AlignedVQ executes layers in the first transformer block and the quantization operation on the edge device. Layers executed on edge requires approximately 7.25 GMACs, while the quantization operation adds 3.63 GMACs, accounting for 2.17% of the entire LLaVA vision encoder (167.45 GMACs). The execution overhead of the compression takes 4.91ms per sample locally, accounting for 25% of the local execution time.

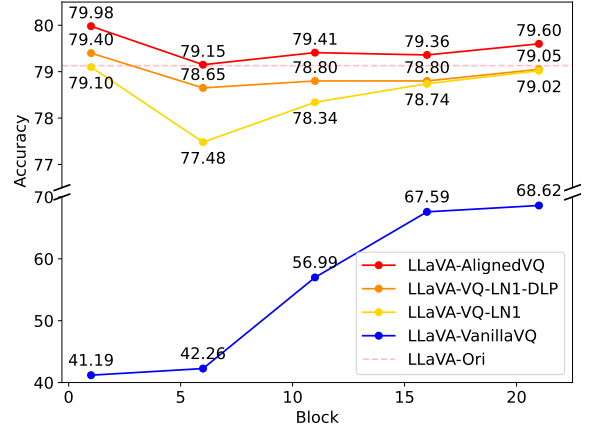


Figure 7: Accuracy improvements across partitioning points achieved through the three proposed design features in AlignedVQ, resulting in variants LLaVA-VQ-LN1, LLaVA-VQ-LN1-DLP, and LLaVA-AlignedVQ. Each design incrementally enhances accuracy compared to LLaVA-VanillaVQ, with gains of 10.4–37.91%, 0.03–1.17%, and 0.5–0.61% respectively. Together, these designs enable LLaVA-AlignedVQ to reach, and in some cases, surpass the accuracy of the original model (LLaVA-Ori).

4.5 Ablation Study

Impacts of Partitioning at Different Blocks. The red curve in Figure 7 shows the impact of different partitioning points (blocks 1, 6, 11, 16, and 21) on the task accuracy of LLaVA-AlignedVQ. As discussed in Section 3.3, transformer models maintain identical computational overhead and intermediate feature sizes across blocks, making early partitioning the optimal strategy for minimizing latency. In this context, *AlignedVQ* provides a two-in-one solution by preserving accuracy performance while achieving the lowest inference latency when applied to the first transformer block.

Importance of AlignedVQ’s Design Features. AlignedVQ has three design features including compressing normalized features after layer normalization layers, aligning features using Dual Linear Project (DLP) module, and including LoRA parameters in the finetuning. Figure 7 illustrates each design feature’s importance by comparing LLaVA-AlignedVQ with the following variants. (1) LLaVA-VQ-LN1-DLP: does not finetune LoRA parameters during the 1-epoch fine-tuning; (2) LLaVA-VQ-LN1 further excludes the DLP module; (3) LLaVA-VanillaVQ applies VQ after a transformer block (i.e., after the FFN layer instead of after the first normalization layer). Compared to the baseline LLaVA-VanillaVQ, applying VQ on normalized intermediate features improves the vanilla VQ accuracy by 10.4 – 37.91%, adding Dual Linear Projection provides an additional 0.03 – 1.17% accuracy boost, and post-

Table 4: The impact of using more codebooks and groups on the task accuracy of LLaVA-AlignedVQ.

#Codebook	1				2	3
#Group	1	2	4	8	1	
LLaVA-AlignedVQ	79.98	79.94	79.96	79.95	79.98	79.99

finetuning the LoRA parameters further increases accuracy by 0.5 – 0.61%.

Impacts of the Number of Codebooks and Groups. LLaVA-AlignedVQ uses the Vanilla VQ with a single codebook and one group. Here, we examine the effect of adding more codebooks and groups in AlignedVQ by incorporating Residual VQ (Zeghidour et al., 2021) and Grouped VQ (Yang et al., 2023) on the task performance of LLaVA-AlignedVQ. Table 4 shows that increasing the number of codebooks and groups yields no or minimal accuracy improvement but results in increased transmission overhead, which scales proportionally with the number of codebooks and groups. Therefore, adding more codebooks and groups is unnecessary in LLaVA-AlignedVQ.

5 RELATED WORK

Vision Language Models (VLMs). VLMs (Alayrac et al., 2022; Li et al., 2023a; Chung et al., 2024) typically consist of a vision encoder to process images, a pretrained Large Language Model (LLM) to handle text, and a multimodal alignment module that bridges the two modalities, allowing the model to understand and generate responses based on both visual and textual inputs. LLaVA-1.5 (Liu et al., 2024a) is one of the state-of-the-art VLMs designed with simple structure and outstanding performance, which is our focus in this paper. It employs a pretrained CLIPViT (Radford et al., 2021) as the vision encoder, an MLP projection for aligning visual and textual information, and a well-trained Vicuna (Chiang et al., 2023) with a LoRA adaptor for generating answers. Although large models achieve impressive results in understanding and generating multimodal content, their computational and memory demands make them impractical for resource-constrained edge devices. To address these limitations, model partitioning offers a potential solution, where part of the model’s computation is offloaded to the cloud. In this paper, we analyze the challenges of partitioning VLMs and propose AlignedVQ, a module that can be integrated into the vision encoder of a pretrained VLM.

Model Partitioning. Model partitioning is a strategy that distributes the computational workload of deep neural networks between edge devices and cloud servers, optimizing metrics such as latency, energy consumption, and resource utilization. One common problem in partitioned execution is to find out the best partition point given a DNN model.

Pioneer work (Teerapittayanon et al., 2017; Kang et al., 2017) profile the energy consumption and total latency of the model to identify such a best point. Meanwhile, some works (Choi & Bajić, 2018; Cohen et al., 2020; Huang et al., 2020; Itahara et al., 2021) pay attention to the intermediate features when split the models across the edge and cloud. (Choi & Bajić, 2018; Cohen et al., 2020) utilize the lossy compression techniques to compress the intermediate features. (Huang et al., 2020) enables the features robust to the network dynamics which can affect the performance of split models on the clouds. However, transformer-based models pose greater challenges for partitioning due to their computational complexity and large intermediate feature sizes, making the intermediate feature compression be important and necessary. To the best of our knowledge, transformer partitioning, particularly in the context of edge-cloud VLMs, remains underexplored, making our work a significant contribution to the field.

Vector Quantization (VQ). VQ has been widely adopted in neural networks particularly for data compression, regularization, and efficient representation learning. For example, VQ-VAE (Van Den Oord et al., 2017) and VQGAN (Esser et al., 2021) introduced VQ into Variational AutoEncoders (VAE) and Generative Adversarial Networks respectively, allowing the model to learn discrete latent representations that compress data more efficiently. The quantization process also acts as a form of regularization, preventing the model from overfitting and encouraging it to learn meaningful features. VQ has also been leveraged for model compression by quantizing neural network weights to extremely low bit-widths, significantly reducing model size without sacrificing performance (Stock et al., 2020; Deng et al., 2024; Liu et al., 2024c). In this paper, we explore the potential of using VQ in model partitioning of VLMs, especially quantizing the intermediate features, which enables efficient edge-cloud collaboration with low transmission overhead while maintaining accuracy.

6 CONCLUSION

We presented AlignedVQ (Aligned Vector Quantization) as a lightweight and effective compression algorithm designed to reduce the transmission overhead of intermediate features while maintaining accuracy in edge-cloud collaborative Vision-Language Models (VLMs). Our experiments showed that AlignedVQ reduces the intermediate feature size of the vision encoder of the pre-trained LLaVA-1.5 model by $1356\times$ while preserving VQA task accuracy. This significant data size reduction can help shorten inference latency in the VLMs system. Future work will focus on extending AlignedVQ’s effectiveness to other large-scale models and further optimizing performance across diverse deployment environments.

REFERENCES

- Abdi, H. Coefficient of variation. *Encyclopedia of research design*, 1(5):169–171, 2010.
- Achiam, J., Adler, S., Agarwal, S., Ahmad, L., Akkaya, I., Aleman, F. L., Almeida, D., Altenschmidt, J., Altman, S., Anadkat, S., et al. Gpt-4 technical report. *arXiv preprint arXiv:2303.08774*, 2023.
- Alayrac, J.-B., Donahue, J., Luc, P., Miech, A., Barr, I., Hasson, Y., Lenc, K., Mensch, A., Millican, K., Reynolds, M., et al. Flamingo: a visual language model for few-shot learning. *Advances in neural information processing systems*, 35:23716–23736, 2022.
- Berahmand, K., Daneshfar, F., Salehi, E. S., Li, Y., and Xu, Y. Autoencoders and their applications in machine learning: a survey. *Artificial Intelligence Review*, 57(2): 28, 2024.
- Chiang, W.-L., Li, Z., Lin, Z., Sheng, Y., Wu, Z., Zhang, H., Zheng, L., Zhuang, S., Zhuang, Y., Gonzalez, J. E., et al. Vicuna: An open-source chatbot impressing gpt-4 with 90%* chatgpt quality. See <https://vicuna.lmsys.org> (accessed 14 April 2023), 2(3):6, 2023.
- Choi, H. and Bajić, I. V. Deep feature compression for collaborative object detection. In *2018 25th IEEE International Conference on Image Processing (ICIP)*, pp. 3743–3747. IEEE, 2018.
- Chung, H. W., Hou, L., Longpre, S., Zoph, B., Tay, Y., Fedus, W., Li, Y., Wang, X., Dehghani, M., Brahma, S., et al. Scaling instruction-finetuned language models. *Journal of Machine Learning Research*, 25(70):1–53, 2024.
- Cohen, R. A., Choi, H., and Bajić, I. V. Lightweight compression of neural network feature tensors for collaborative intelligence. In *2020 IEEE International Conference on Multimedia and Expo (ICME)*, pp. 1–6. IEEE, 2020.
- Deng, J., Li, S., Wang, Z., Gu, H., Xu, K., and Huang, K. Vq4dit: Efficient post-training vector quantization for diffusion transformers. *arXiv preprint arXiv:2408.17131*, 2024.
- Esser, P., Rombach, R., and Ommer, B. Taming transformers for high-resolution image synthesis. In *Proceedings of the IEEE/CVF conference on computer vision and pattern recognition*, pp. 12873–12883, 2021.
- Gersho, A. and Gray, R. M. *Vector quantization and signal compression*, volume 159. Springer Science & Business Media, 2012.
- Goyal, Y., Khot, T., Summers-Stay, D., Batra, D., and Parikh, D. Making the v in vqa matter: Elevating the role of image understanding in visual question answering. In *Proceedings of the IEEE conference on computer vision and pattern recognition*, pp. 6904–6913, 2017.
- Gurari, D., Li, Q., Stangl, A. J., Guo, A., Lin, C., Grauman, K., Luo, J., and Bigham, J. P. Vizwiz grand challenge: Answering visual questions from blind people. In *Proceedings of the IEEE conference on computer vision and pattern recognition*, pp. 3608–3617, 2018.
- Huang, J., Samplawski, C., Ganesan, D., Marlin, B., and Kwon, H. Clio: Enabling automatic compilation of deep learning pipelines across iot and cloud. In *Proceedings of the 26th Annual International Conference on Mobile Computing and Networking*, pp. 1–12, 2020.
- Hudson, D. A. and Manning, C. D. Gqa: A new dataset for real-world visual reasoning and compositional question answering. In *Proceedings of the IEEE/CVF conference on computer vision and pattern recognition*, pp. 6700–6709, 2019.
- Itahara, S., Nishio, T., and Yamamoto, K. Packet-loss-tolerant split inference for delay-sensitive deep learning in lossy wireless networks. *arXiv preprint arXiv:2104.13629*, 2021.
- Kang, Y., Hauswald, J., Gao, C., Rovinski, A., Mudge, T., Mars, J., and Tang, L. Neurosurgeon: Collaborative intelligence between the cloud and mobile edge. In *ACM SIGARCH Computer Architecture News*, volume 45, pp. 615–629. ACM, 2017.
- Kingma, D. P. Adam: A method for stochastic optimization. *arXiv preprint arXiv:1412.6980*, 2014.
- Li, J., Li, D., Savarese, S., and Hoi, S. Blip-2: Bootstrapping language-image pre-training with frozen image encoders and large language models. In *International conference on machine learning*, pp. 19730–19742. PMLR, 2023a.
- Li, Y., Du, Y., Zhou, K., Wang, J., Zhao, W. X., and Wen, J.-R. Evaluating object hallucination in large vision-language models. *arXiv preprint arXiv:2305.10355*, 2023b.
- Lin, H., Bai, H., Liu, Z., Hou, L., Sun, M., Song, L., Wei, Y., and Sun, Z. Mope-clip: Structured pruning for efficient vision-language models with module-wise pruning error metric. In *Proceedings of the IEEE/CVF Conference on Computer Vision and Pattern Recognition*, pp. 27370–27380, 2024.
- Lin, T.-Y., Maire, M., Belongie, S., Hays, J., Perona, P., Ramanan, D., Dollár, P., and Zitnick, C. L. Microsoft coco: Common objects in context. In *Computer Vision—ECCV 2014: 13th European Conference, Zurich, Switzerland, September 6–12, 2014, Proceedings, Part V 13*, pp. 740–755. Springer, 2014.

- Liu, H., Li, C., Wu, Q., and Lee, Y. J. Visual instruction tuning. *Advances in neural information processing systems*, 36, 2023.
- Liu, H., Li, C., Li, Y., and Lee, Y. J. Improved baselines with visual instruction tuning. In *Proceedings of the IEEE/CVF Conference on Computer Vision and Pattern Recognition*, pp. 26296–26306, 2024a.
- Liu, H., Li, C., Li, Y., Li, B., Zhang, Y., Shen, S., and Lee, Y. J. Llava-next: Improved reasoning, ocr, and world knowledge, January 2024b. URL <https://llava-vl.github.io/blog/2024-01-30-llava-next/>.
- Liu, Y., Wen, J., Wang, Y., Ye, S., Zhang, L. L., Cao, T., Li, C., and Yang, M. Vptq: Extreme low-bit vector post-training quantization for large language models. *arXiv preprint arXiv:2409.17066*, 2024c.
- Liu, Y., Duan, H., Zhang, Y., Li, B., Zhang, S., Zhao, W., Yuan, Y., Wang, J., He, C., Liu, Z., et al. Mmbench: Is your multi-modal model an all-around player? In *European Conference on Computer Vision*, pp. 216–233. Springer, 2025.
- Radford, A., Kim, J. W., Hallacy, C., Ramesh, A., Goh, G., Agarwal, S., Sastry, G., Askell, A., Mishkin, P., Clark, J., et al. Learning transferable visual models from natural language supervision. In *International conference on machine learning*, pp. 8748–8763. PMLR, 2021.
- Singh, A., Natarajan, V., Shah, M., Jiang, Y., Chen, X., Batra, D., Parikh, D., and Rohrbach, M. Towards vqa models that can read. In *Proceedings of the IEEE/CVF conference on computer vision and pattern recognition*, pp. 8317–8326, 2019.
- Singh, H. J., Bathla, G., Mehta, M., Chhabra, G., and Singh, P. Visual questions answering developments, applications, datasets and opportunities: A state-of-the-art survey. In *2023 International Conference on Sustainable Computing and Data Communication Systems (ICSCDS)*, pp. 778–785. IEEE, 2023.
- Stock, P., Joulin, A., Gribonval, R., Graham, B., and Jégou, H. And the bit goes down: Revisiting the quantization of neural networks. In *ICLR 2020-Eighth International Conference on Learning Representations*, pp. 1–11, 2020.
- Teerapittayanon, S., McDanel, B., and Kung, H.-T. Distributed deep neural networks over the cloud, the edge and end devices. In *2017 IEEE 37th International Conference on Distributed Computing Systems (ICDCS)*, pp. 328–339. IEEE, 2017.
- Van Den Oord, A., Vinyals, O., et al. Neural discrete representation learning. *Advances in neural information processing systems*, 30, 2017.
- Yang, D., Liu, S., Huang, R., Tian, J., Weng, C., and Zou, Y. Hifi-codec: Group-residual vector quantization for high fidelity audio codec. 2023.
- Yu, W., Yang, Z., Li, L., Wang, J., Lin, K., Liu, Z., Wang, X., and Wang, L. Mm-vet: Evaluating large multi-modal models for integrated capabilities. *arXiv preprint arXiv:2308.02490*, 2023.
- Zeghidour, N., Luebs, A., Omran, A., Skoglund, J., and Tagliasacchi, M. Soundstream: An end-to-end neural audio codec, 2021.